Dentomaxillofacial Radiology (2017) 46, 20170030

birpublications.org/dmfr

RESEARCH ARTICLE

Head and neck effective dose and quantitative assessment of image quality: a study to compare cone beam CT and multislice spiral CT

[1]Cosimo Nardi, [2]Cinzia Talamonti, [2]Stefania Pallotta, [3]Paola Saletti, [1]Linda Calistri, [1]Cesare Cordopatri and [1]Stefano Colagrande

[1]Department of Experimental and Clinical Biomedical Sciences, Radiodiagnostic Unit n. 2, University of Florence—Azienda Ospedaliero-Universitaria Careggi, Florence, Italy; [2]Department of Experimental and Clinical Biomedical Sciences, Medical Physics Unit, University of Florence—Azienda Ospedaliero-Universitaria Careggi, Florence, Italy; [3]Department of Health Directorate, UOC Health Physics Unit, University of Florence—Azienda Ospedaliero-Universitaria Careggi, Florence, Italy

Objectives: To evaluate the effective dose and image quality of horizontal CBCT in comparison with multislice spiral CT (MSCT) in scans of the head, cervical spine, ear and dental arches.
Methods: A head and neck Alderson-Rando® phantom (The Phantom Laboratory, Salem, NY) equipped with 74 thermoluminescence dosemeters was exposed according to 5 different scans in CBCT and 4 different scans in MSCT. Spatial and contrast resolutions, in terms of modulation transfer function and contrast-to-noise ratio (CNR), were measured to obtain a quantitative assessment of image quality.
Results: The CBCT effective dose was 248, 249, 361, 565 and 688 μSv in the cervical spine, head, ear, dental arches with small field of view and dental arches with medium field of view, respectively. The MSCT effective dose was 3409, 1892, 660 and 812 μSv in the cervical spine, head, ear and dental arches, respectively. The modulation transfer function was 0.895 *vs* 0.347, 0.895 *vs* 0.275, 0.875 *vs* 0.342 and 0.961 *vs* 0.352 for CBCT *vs* MSCT in the cervical spine, head, ear and dental arches, respectively. Head and cervical spine MSCT showed greater CNR than CBCT, whereas CNR of the ear and dental arches showed comparable values.
Conclusions: CBCT was preferable to MSCT for the ear and dental arches volumetric imaging due to its lower radiation dose and significantly higher spatial resolution. In the case of cervical spine and head imaging, MSCT should be generally recommended if a high contrast resolution is required, despite the greater radiation exposure.
Dentomaxillofacial Radiology (2017) **46**, 20170030. doi: 10.1259/dmfr.20170030

Cite this article as: Nardi C, Talamonti C, Pallotta S, Saletti P, Calistri L, Cordopatri C, et al. Head and neck effective dose and quantitative assessment of image quality: a study to compare cone beam CT and multislice spiral CT. *Dentomaxillofac Radiol* 2017; **46**: 20170030.

Keywords: CBCT; radiation exposure; effective dose; spatial/contrast resolution; image quality

Introduction

In recent years, employment of diagnostic radiography has increased progressively, and at the same time, the cancer risk induced by multislice spiral CT (MSCT) scans seems to have increased.[1] CBCT is a relatively new imaging technique that has recently emerged in the field of radiodiagnostics. It utilizes a conic/pyramidal X-ray beam which hits a two-dimensional detector

Correspondence to: Dr Cosimo Nardi. E-mail: cosimo.nardi@unifi.it
Received 26 January 2017; revised 28 April 2017; accepted 15 May 2017

(image intensifier or flat panel) during a lengthy single rotation (5.4–40 s).[2] The reduced presence of metal artefacts and the high spatial resolution (0.075–0.4 mm isotropic voxel) have made CBCT a technique widely used not only in dentomaxillofacial radiology[3] but also for cervical spine and middle ear imaging.[4]

Many studies investigated head/dental CBCT effective dose and dosimetric differences between MSCT and CBCT.[5–9] They proved that the CBCT effective dose is undoubtedly lower than the MSCT dose, regardless of the broad variability in CBCT dose resulting from the appliance and the protocol employed.

However, only few studies concerning the head and neck area tried to establish a relationship between effective dose and quantitative measurement of image quality.[6,10–12] Moreover, there are only three works on ear dose,[10,13,14] and no article exists regarding spine dose.

The aim of this study was to evaluate the effective dose and image quality of horizontal CBCT in comparison with MSCT in the scans of the head, cervical spine, ear and dental arches (concurrently the upper and lower jaws).

Methods and materials

Devices and protocols

Scans were carried out *via* SOMATOM® Sensation 64 MSCT (Siemens, Erlangen, Germany) and NewTom™5G CBCT (QR srl, Verona, Italy). The latter was equipped with a pulsed pyramidal X-ray beam (360° of rotation), a very small focal spot (0.3 mm) and an amorphous silicon flat-panel detector (20 × 25 cm). In addition, it embedded the SafeBeam™. This technology features the use of intermittent bursts of radiation (ms) and automatically adjusts the radiation dosage by modifying the tube current (mA) according to pre-set dose levels determined by the patient's size as measured on the scout images.

All technical/geometrical parameters were the same as those used in the clinical practice (Table 1). Since even small modifications in the size and position of field of view (FOV) heavily influenced the effective dose, an accurate positioning of FOV was mandatory (Figure 1).

In CBCT, the FOV of the head was the widest available (18 × 16 cm). It was placed so that the soft tissues of the nose and chin were completely included to fulfil the clinician's requirements for orthognathodontic treatment/surgical planning; the cranial vertex and occipital bone were thus excluded. In MSCT, the FOV of the head included the entire skull since scanning the head for orthognathodontic purposes is not recommended due to the high radiation dose.[7,15] The FOV of the cervical spine, ear and dental arches was kept as similar as possible between both devices whilst still trying to maintain the standard settings. CBCT of dental arches was studied with two different FOVs: small (8 × 8 cm) and medium (12 × 8 cm). It is important to remind that an exact dosimetric match between CBCT and MSCT is only achievable when the FOV of CBCT completely includes the scanned object. In MSCT, the diameter of the X-ray beam always covers the entire object, therefore only the scan length is relevant from a dosimetric point of view.

NewTom5G exposure parameters could not be altered by the operator and were automatically set in relation to the FOV, radiographic absorption and available acquisition protocol. The two protocols chosen—named standard-regular and high-resolution (hi-res) enhanced by the producer—lasted 18 and 36 s, and included 360 and 480 basis image frames, respectively. The protocol was chosen accordingly to the diagnostic application. The ear and dental arches were acquired with smaller voxels and greater mA (hi-res-enhanced protocol) than the head and cervical spine (standard-regular protocol) to better depict fine anatomical structures such as ossicular chain in ear study or neurovascular canal in dental extractive/implant planning. Both CBCT and MSCT scans were performed at normal dose settings, except for scans of the dental arches with MSCT, which were conducted at significantly reduced dose settings by decreasing mAs value (low-dose Dentascan).[16]

Phantom and experimental setup

An adult male Alderson-Rando® anthropomorphic phantom (The Phantom Laboratory, Salem, NY) was used. The phantom consisted of a real human skeleton filled with tissue equivalent material according to The International Commission on Radiation Units and Measurements-44 specification, transected horizontally into 2.5-cm-thick slices from the head vertex to the groin. For the current study, only the upper 12 slices (*i.e.* head and neck) were used. Each slice had cylindrical drilled holes in default locations that were plugged with two lithium fluoride (LiF:Mg,Ti) thermoluminescence dosemeter (TLD-100™ rods; Harshaw Chemical Company, Solon, OH) chips (3.2 × 3.2 × 0.5 mm) to measure radiation exposure. The holes used for the measurements were chosen among those that more accurately represented the anatomical location of the organs of interest (Table 2). The dosimetric response for each hole was calculated as the arithmetic mean of the two thermoluminescence dosemeter (TLD) chip exposures. 37 anatomical sites were considered for both CBCT and MSCT, thereby 74 TLDs were used for each scan. Consequently, a total of 370 and 296 dosemeters were used in the 5 CBCT and 4 MSCT scans, respectively. The TLD response was well above the background dose and also showed low variability in each phantom hole. For this reason, only one exposure was performed for each technique and therefore no scan was repeated.

The phantom was always positioned with a headrest as if it were a real patient, so that

– the occlusal plane was perpendicular to the patient table

Table 1 CBCT (standard-regular protocol) and multislice spiral CT (MSCT) exposure parameters about the head, cervical spine, ear and dental arches

Device	*Anatomical area*	*Tube voltage (kV)*	*CTDIvol*[a] *(mGy)*	*DLP (mGy cm)*	*DAP (mGy cm²)*	*Air kerma (mGy)*	*Current × exposure time (mAs)*	*Rotation time*[b] *(s)*	*Scan diameter (cm)*	*Scan length (cm)*	*Reconstruction FOV (AP, LL × CC) (cm cm)*	*Reconstruction kernel*	*Voxel side (mm)*	*Pixel size*[c] *(mm)*	*Slice thickness (mm)*	*Pitch (mm)*
CBCT	Head	110	2.49	39.87	794.87	3.75	10.23	18	18	16	18 × 16	—	0.30	—	—	—
	Cervical spine	110	2.84	45.39	904.85	4.27	13.08	18	18	16	18 × 16	—	0.30	—	—	—
	Ear	110	20.57	128.57	1835.18	29.10	141.92	36	15	5	15 × 5	—	0.15	—	—	—
	Dental arches	110	10.53	94.80	1502.40	17.41	77.60	36	12	8	12 × 8	—	0.15	—	—	—
	Dental arches	110	7.44	66.98	1006.42	14.85	63.80	36	8	8	8 × 8	—	0.15	—	—	—
MSCT	Head	120	23.24	553.00	—	—	150	—	—	22	24 × 22	H40s medium	—	0.34	4.80	—
	Cervical spine	120	13.49	314.33	—	—	200	1	—	18	12 × 18	B40s medium	—	0.39	2.00	0.90
	Ear	120	36.94	317.69	—	—	120	1	—	6	15 × 6	U90u ultra sharp	—	0.41	2.00	0.85
	Dental arches	120	12.53	173.53	—	—	80	1	—	10	15 × 10	H60s sharp	—	0.39	0.60	0.90

AP, anteroposterior diameters; CC, craniocaudal diameters; CTDI, CT dose index; DAP, dose–area product; DLP, dose–length product; FOV, field of view; LL, laterolateral diameters. Size of AP and LL was equal.

The protocols were optimized in such a way as to simulate the routine clinical practice. Since the acquisition was performed in a sequential manner, no rotation time and pitch value have been indicated for the MSCT head scan.

[a]$CTDI_{vol}$ values are referenced to a 16-cm-diameter CTDI phantom.

[b]The rotation time was the time for each 360° rotation. In CBCT, the rotation time corresponds to the full scan time.

[c]The pixel size was measured in the axial plane.

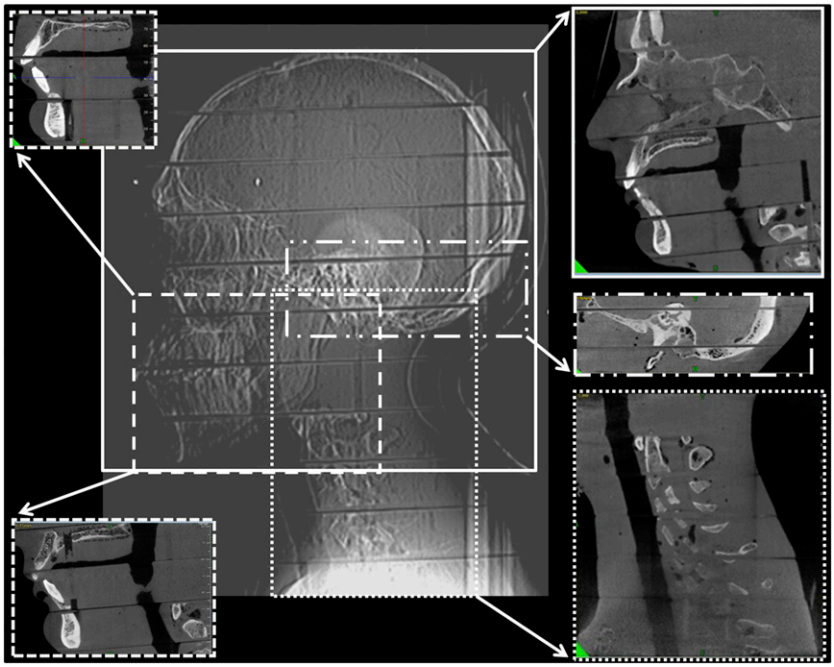

Figure 1 Overview of all fields of view (FOVs). The multislice spiral CT FOVs are represented in the middle of the picture. The corresponded FOVs used in CBCT are showed on the edge of the picture.

– the midheight/midsagittal plane was centred on the horizontal/vertical positioning light beam
– the midsagittal plane was aligned with the midline of the gantry.

Dosimetric method and effective dose calculation

Dosimetric evaluation[17] was performed with TLDs. On irradiated fraction, the collected charge in the TLD was read in a regularly calibrated automatic nitrogen flow Harshaw 5500 reader (Harshaw Chemical Company). The background dose was estimated by using non-irradiated TLDs and subtracted from all the TLD measured values. The following equation was used to calculate the mean equivalent dose or radiation weighted dose H_T for all organs or tissues T:

$$H_T = W_R \sum_i f_i D_{Ti}$$

where W_R is the radiation weighting factor (1 for X-rays), f_i is the irradiated fraction of the tissue T in the slice i and D_{Ti} is the mean absorbed dose of tissue/organ T in slice i (Table 2).

As described by Golikov and Nikitin,[18] each organ in the phantom, except bone, was a homogeneous soft-tissue organ, therefore the mass fraction to volume fraction ratio was 1. The Golikov and Nikitin's method was used by Scalzetti et al[19] to determine the mass fraction for the organs at risk.

The salivary glands, thyroid gland, brain, extrathoracic airways and oral mucosa were entirely within the head and neck area (100% irradiated fraction), whereas the oesophagus, skin, lymphatic nodes, muscles, bone marrow and bone surface were only partially included. The extrathoracic airways, oral mucosa, lymphatic nodes and muscles formed part of the remainder tissues. The head and neck area included 10% of the oesophagus and 5% of the skin, muscles and lymphatic nodes with respect to the total body amount of these organs.[5] In the case of a 40-year-old patient, 7.6%, 0.8% and 3.9% of the whole body's active bone marrow resides in the cranium, mandible and cervical spine, respectively.[20]

The bone surface was calculated as the percentage of fresh skull, mandible and cervical spine over the total fresh skeletal mass[21] (the mass of cervical vertebrae was estimated as being 7/34 of total vertebral mass). The trabecular component percentage was then subtracted from the total skeletal mass to obtain the cortical portion.[22]

The effective dose was determined by the equation:

$$E = \sum_i W_T H_T$$

where Σ represents the sum of the products of the tissue weighting factors (W_T)—established by the International Commission on Radiological Protection[23]—and the absorbed dose within that tissue H_T. For instance, the contribution of the oesophagus to the effective dose, as well as for the other organs, was calculated by multiplying its absorbed dose by the oesophageal irradiated fraction (0.1); the resulting value was multiplied by the weight factor of the oesophagus (0.04).

Image quality

Quantitative assessment of image quality was implemented by measuring spatial and contrast resolution, represented by modulation transfer function (MTF) and

Table 2 Tissue weighting factors (W_T), fractions irradiated (f_i) and dosemeters (number and location) used to calculate the effective dose

Organ	W_T	f_i	*Number of TLD*	*Slice*
Lens of eye			1–4	4
Right lens of eye			1, 2	4
Left lens of eye			3, 4	4
Ossicles chain			5–8	5
Right ossicles chain			5, 6	5
Left ossicles chain			7, 8	5
Thyroid	0.04	1	9–12	9
Thyroid—right			9, 10	9
Thyroid—left			11, 12	9
Salivary glands	0.01	1	13–22	7, 8
Right submandibular gland			13, 14	8
Left submandibular gland			15, 16	8
Right parotid			17, 18	7
Left parotid			19, 20	7
Centre sublingual gland			21, 22	8
Bone marrow	0.12	0.123	23-28, 33–36, 41-46	2, 3, 6, 7, 8, 9
Calvaria/skull base		0.076	23-28, 45, 46	2, 3, 6
Calvarium anterior			23, 24	2
Calvarium posterior			25, 26	3
Calvarium right			27, 28	3
Skull base			45, 46	6
Mandible		0.008	33–36	8
Mandible right (trabecular)			33, 34	8
Mandible left (trabecular)			35, 36	8
Cervical spine		0.039	41–44	7, 9
Cervical spine C2 (trabecular)			41, 42	7
Cervical spine C4 (trabecular)			43, 44	9
Bone surface	0.01	0.133	23-32, 37-40	2, 3, 7, 8, 9
Calvaria		0.112	23–28	2, 3
Calvarium anterior			23, 24	2
Calvarium posterior			25, 26	3
Calvarium right			27, 28	3
Mandible		0.011	29–32	8
Mandible right (cortical)			29, 30	8
Mandible left (cortical)			31, 32	8
Cervical spine		0.010	37–40	7, 9
Cervical spine C2 (cortical)			37, 38	7
Cervical spine C4 (cortical)			39, 40	9
Brain	0.01	1	47–50	3, 4
Pituitary gland			47, 48	4
Mid-brain			49, 50	3
Oesophagus	0.04	0.1	51, 52	9
Skin	0.01	0.05	53–56	6, 7
Skin—right cheek			53, 54	6
Skin—back of the neck			55, 56	7
Extrathoracic airway	0.0086	1	57–62	4, 5, 7
Oropharyngeal airway			57, 58	7
Right maxillary sinus			59, 60	5
Left ethmoid			61, 62	4
Oral mucosa	0.0086	1	63, 64	6
Lymph nodes	0.0086	0.05	65–68	9
Right laterocervical lymph nodes			65, 66	9
Left laterocervical lymph nodes			67, 68	9
Muscles	0.0086	0.05	69–74	5, 6, 8
Right cutaneous muscles			69, 70	6
Left masticatory muscle			71, 72	5
Back of the neck muscles			73, 74	8

TLD, thermoluminescence dosemeter.
Extrathoracic airways, oral mucosa, lymphatic nodes and muscles form part of the remainder tissues.

contrast-to-noise ratio (CNR, contrast resolution), respectively.[24] CNR and MTF were considered together when interpreting the image quality.

Spatial resolution was measured with a CATPHAN® 504 phantom (The Phantom Laboratory), a cylindrical phantom consisting of five modules enclosed in a 20-cm plastic housing that is employed for quality assurance of CT scanners (http://www.phantomlab.com). A hi-res module containing a point source was scanned for all MSCT and CBCT protocols. All data sets were exported in digital imaging and communications in medicine format and assessed with a customized version of

MATLAB® (MathWorks®, Natick, MA; https://www.mathworks.com/products/matlab.html) to calculate the MTF. The MTF is given by the Fourier transform of the point spread function, a delta function which describes the imaging system response to a point input. The ideal MTF is independent from the spatial frequency and corresponds to the point spread function. A broader point spread function corresponds to a narrower MTF and a greater loss of high spatial frequency information. In the present study, the MTF was evaluated at 50% frequency cut-off, since MTF evaluation at 10% frequency cut-off was unachievable in some acquisitions.

Owing to the limited size of the FOV, the CNR evaluation in CBCT required the use of a special phantom obtained by assembling five tissue substitute plugs of different certified materials (Gammex RMI®, Middelton, WI) with electron density relative to water ranging from 1.018 to 1.82 g cm^{-3}. The phantom was scanned for every CBCT and MSCT protocol, and the images were processed using ImageJ[25] (a public domain, Java-based open architecture source code developed at the National Institutes of Health, https://imagej.nih.gov/ij). The mean values and standard deviations for the regions of interest set on each insert were calculated to evaluate the CNR, according to the following definition:

$$\mathrm{CNR}_i = \frac{I_i - I_{\mathrm{we}}}{\sqrt{\sigma_i^2 + \sigma_{\mathrm{we}}^2}}$$

where I_i , σ_i and I_{we}, σ_{we} represent the mean values and standard deviations for the insert i and for the water equivalent one, respectively. The latter had the lowest contrast with the background.

Results

Dose

The organ dose and effective dose for each anatomical area are illustrated in Tables 3 and 4.

Multislice spiral CT vs *CBCT:* The effective dose measured for CBCT was 7.2%, 13.1%, 54.7%, 69.5% and 84.7% of the effective dose of MSCT in the cervical spine, head, ear, dental arches with small FOV and dental arches with medium FOV, respectively. In CBCT standard-regular protocol for cervical spine and head scans, the most significant difference between the two CT technologies was observed in the thyroid gland. The CBCT thyroid effective dose was 9.1% and 23.0% of MSCT thyroid effective dose for the cervical spine and head scans, respectively. On the contrary, in CBCT hi-res-enhanced protocols (scans of the ear and dental arches), some organs showed the same or almost identical effective dose with respect to MSCT. This is the case for the skin in scans of the ear and for the remainder tissue in scans of the dental arches.

In CBCT, the highest organ doses were those of the ossicular chain (19.0 mGy) and salivary glands (12.0 mGy) in scans of the ear and dental arches, respectively. In MSCT, the highest organ dose affected the thyroid gland (49.0 mGy) in the cervical spine scan, followed by the eye lens (42.3 mGy) and ossicular chain (37.7 mGy) in ear scan.

Cervical spine scan: The thyroid gland contributed the most to the effective dose (57.5% in MSCT and 71.8% in CBCT).

Head scan: In MSCT, the thyroid gland, bone marrow and remainder tissues provided around 21.5% of the effective dose, each. In CBCT, the thyroid gland

Table 3 Absorbed dose, effective dose and the contribution ($W_T H_T$) of the dose of each organ/tissue to the cervical spine and head effective doses

	Cervical spine					*Head*				
	Absorbed dose (mGy)		*$W_T H_T$ (μSv, %)*			*Absorbed dose (mGy)*		*$W_T H_T$ (μSv, %)*		
Tissue/organ	*MS*	*CB*	*MS*	*CB*	*CB/MS*	*MS*	*CB*	*MS*	*CB*	*CB/MS*
Lens of eye	27.3	1.1				30.8	4.2			
Ossicles chain	19.1	0.1				28.1	3.1			
Thyroid gland	49.0	4.4	1960 (57.5%)	178 (71.8%)	9.1%	10.0	2.3	400 (21.1%)	92 (36.7%)	23.0%
Salivary glands	32.0	2.5	320 (9.4%)	26 (10.5%)	8.1%	30.7	3.6	307 (16.2%)	36 (14.5%)	11.7%
Bone marrow	4.0	0.2	488 (14.3%)	29 (11.7%)	5.9%	3.4	0.3	409 (21.6%)	41 (16.5%)	10.0%
Bone surface	3.4	0.2	34 (1.0%)	3 (1.2%)	8.8%	2.8	0.3	28 (1.5%)	3 (1.2%)	10.7%
Brain	9.0	0.1	90 (2.6%)	1 (0.4%)	1.1%	22.7	1.2	228 (12.0%)	13 (5.2%)	5.7%
Oesophagus	2.9	0.1	116 (3.4%)	3 (1.2%)	2.6%	2.3	0.2	93 (4.9%)	11 (4.4%)	11.8%
Skin	1.3	0.1	13 (0.4%)	1 (0.4%)	7.6%	1.2	0.1	13 (0.7%)	2 (0.8%)	12.0%
RT EA	22.3	0.4	192 (5.7%)	3 (1.2%)	1.5%	20.5	3.1	177 (9.4%)	27 (10.8%)	15.3%
Oral mucosa	20.0	0.2	172 (5.1%)	2 (0.8%)	1.1%	24.5	2.4	211 (11.2%)	21 (8.4%)	9.9%
Lymph nodes	1.4	0.1	12 (0.3%)	1 (0.4%)	8.3%	1.6	0.2	14 (0.7%)	2 (0.8%)	14.2%
Muscles	1.4	0.1	12 (0.3%)	1 (0.4%)	8.3%	1.4	0.2	12 (0.6%)	1 (0.4%)	8.3%
Total	45.1	0.8	388 (11.4%)	7 (2.8%)	1.8%	48.0	5.9	414 (21.9%)	51 (20.5%)	12.3%
Effective dose [μSv]	—	—	3409 (100%)	248 (100%)	7.2%	—	—	1892 (100%)	249 (100%)	13.1%

CB, CBCT; EA, extrathoracic airways; H_T, equivalent dose; MS, multislice CT; RT, remainder tissues; W_T, tissue weighting factor.
The value of absorbed dose of each organ is already multiplied by its irradiated fraction. All values of the effective dose are approximate.

Table 4 Absorbed dose, effective dose and the contribution ($W_T H_T$) of the dose of each organ/tissue to the ear and dental arches effective doses

	Ear					*Dental Arches*							
	Absorbed dose (mGy)		*$W_T H_T$ (μSv, %)*			*Absorbed dose (mGy)*			*($W_T H_T$) (μSv, %)*				
Tissue/organ	*MS*	*CB*	*MS*	*CB*	*CB/MS*	*MS*	*CBm*	*CBs*	*MS*	*CBm*	*CBm/MS*	*CBs*	*CBs/MS*
Lens of eye	42.3	5.1				9.1	6.7	3.9					
Ossicles chain	37.7	19.0				9.4	7.0	4.1					
Thyroid gland	2.2	0.8	86 (13.0%)	31 (8.6%)	36.0%	5.6	5.4	4.2	226 (27.8%)	216 (31.4%)	95.5%	170 (30.1%)	75.2%
Salivary glands	13.4	9.8	134 (20.3%)	98 (27.1%)	73.1%	14.6	12.0	10.7	146 (18.0%)	120 (17.4%)	82.2%	107 (18.9%)	73.2%
Bone marrow	1.5	0.8	187 (28.3%)	96 (26.6%)	51.3%	1.2	1.0	0.6	142 (17.5%)	117 (17.0%)	82.3%	70 (12.4%)	49.3%
Bone surface	0.7	0.3	8 (1.2%)	3 (0.8%)	37.5%	1.2	1.0	0.7	12 (1.5%)	10 (1.5%)	83.3%	7 (1.2%)	58.3%
Brain	10.4	3.1	104 (15.8%)	31 (8.6%)	29.8%	3.6	0.4	0.5	36 (4.4%)	4 (0.6%)	11.1%	5 (0.9%)	13.8%
Oesophagus	0.4	0.4	16 (2.4%)	12 (3.3%)	75.0%	1.4	0.8	0.7	55 (6.8%)	30 (4.4%)	54.5%	26 (4.6%)	47.2%
Skin	0.5	0.6	5 (0.8%)	6 (1.7%)	120.0%	0.6	0.6	0.5	6 (10.7%)	5 (0.7%)	83.3%	5 (0.9%)	83.3%
RT EA	11.2	8.2	96 (14.6%)	70 (19.4%)	72.9%	9.5	9.5	9.8	81 (10.0%)	81 (11.8%)	100.0%	84 (14.9%)	103.7%
Oral mucosa	1.3	0.8	11 (1.6%)	7 (1.9%)	63.6%	11.8	11.3	10.0	101 (12.4%)	97 (14.1%)	96.0%	86 (15.2%)	85.1%
Lymph nodes	0.1	0.1	1 (0.2%)	0.3 (0.1%)	30.0%	0.4	0.6	0.3	3 (0.4%)	5 (0.7%)	166.6%	3 (0.5%)	100.0%
Muscles	1.4	0.8	12 (1.8%)	7 (1.9%)	58.3%	0.5	0.3	0.3	4 (0.5%)	3 (0.5%)	75.0%	2 (0.3%)	50.0%
Total	14.0	9.9	120 (18.2%)	84 (23.3%)	70.0%	22.2	21.7	20.4	191 (23.5%)	187 (27.1%)	97.9%	175 (30.9%)	91.6%
Effective dose [μSv]	-	-	660 (100%)	361 (100%)	54.7%	-	-	-	812 (100%)	688 (100%)	84.7%	565 (100%)	69.5%

CB, CBCT (high-resolution-enhanced protocol); CBm, CBCT with medium FOV (12 × 8 cm); CBs, CBCT with small FOV (8 × 8 cm); EA, extrathoracic airways; FOV, field of view; H_T, equivalent dose; MS, multislice CT; RT, remainder tissues; W_T, tissue weighting factor.
The value of absorbed dose of each organ is already multiplied by its irradiated fraction. All values of effective dose are approximate.

contributed the most to the effective dose with 36.7%, followed by the remainder tissues and bone marrow with 20.5% and 16.5%, respectively.

Ear scan: The dominant contributions to the effective dose originated from the bone marrow, salivary glands and remainder tissues. They were 28.3%, 20.3% and 18.2% in MSCT; 26.6%, 27.1% and 23.3% in CBCT, respectively.

In addition, the contributing percentage of the brain to the effective dose in ear and head MSCT scans was around twice that of CBCT (15.8% *vs* 8.6% and 12.0% *vs* 5.2%, respectively).

Dental arches scan: The most significant contributions to the effective dose derived from the thyroid gland and remainder tissues (around 25% in MSCT and 30% in CBCT), followed by the bone marrow and salivary glands (17.5% in both MSCT and CBCT).

Image quality

The MTF of CBCT was 0.895, 0.895, 0.875 and 0.961 in the cervical spine, head, ear and dental arches, respectively. The MTF of MSCT was 0.347, 0.275, 0.342 and 0.352 in the cervical spine, head, ear and dental arches, respectively. In Figure 2, 50% cut-offs of the MTFs were reported. The 50% MTF ratios between CBCT and MSCT were 2.6 (cervical spine and ear), 2.7 (dental arches) and 3.3 (head). This demonstrated that CBCT images had better spatial resolution than MSCT for all protocols.

The CNR values, as function of the plugs density, were reported in Figures 3 and 4. At densities around 1 g cm^{-3} (solid water and brain), the CNR showed similar values in MSCT and CBCT whilst at higher densities—*i.e.* between 1 and 2 (inner and cortical bone)—head and cervical spine MSCT showed progressively greater CNR than CBCT. The CNR values were comparable in all the other protocols, even though CBCT showed slightly better values than MSCT.

When MTF and CNR values were considered together, CBCT image quality was higher than MSCT for scans of the ear and dental arches, whereas for head and cervical spine scans, a definite judgment on which CT-technologies had the highest image quality was not possible.

Discussion

In scans of the dental arches, CBCT showed effective dose somewhat below (around three-quarters) and image quality greater for its obvious higher spatial resolution than low-dose Dentascan-MSCT. The same considerations can be applied to the ear study in which the effective dose of CBCT was about half that of MSCT, but the image quality of CBCT was greater

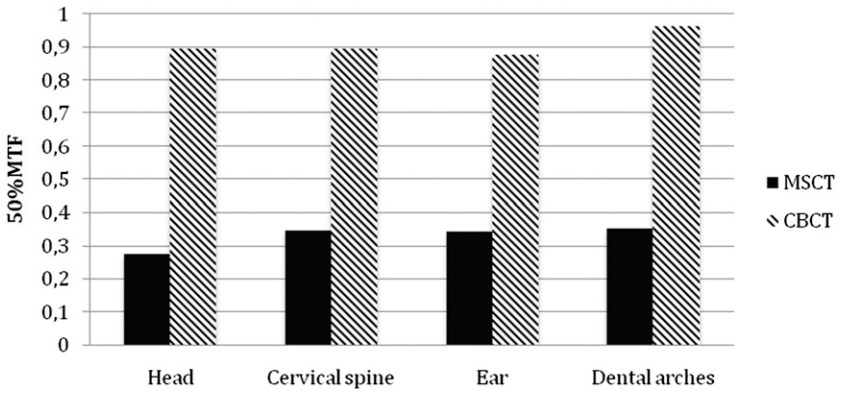

Figure 2 Multislice spiral CT (MSCT) and CBCT values in correspondence of the modulation transfer function (MTF) 50% cut-off for each anatomical area.

thanks to its superior spatial resolution with similar contrast resolution.

In head and cervical spine scans, the effective dose of CBCT was evidently lower (around one-tenth) than MSCT. CBCT showed superior spatial resolution (MTF) but inferior CNR than MSCT. It is not possible to assess the individual contribution of MTF and CNR to the overall image quality, therefore which CT technology has the highest image quality remains unclear in this case. Since the current article focused on the technical quality of the image, it is also worth emphasising that technical and clinical image quality do not always correlate.

In general terms, CBCT has greater spatial resolution than MSCT because it uses flat-panel detectors with thinner scintillator layers and smaller pixels than those of MSCT. Unlike MSCT, in CBCT there is no post-patient collimation. As a result, the image is obtained with fewer photons being wasted, although its quality is degraded by scattered radiation. Both these techniques use the same image reconstruction principle, termed back-projection, with the addition of Feldkamp's algorithm in CBCT.[26] MSCT is characterized by greater mA and wider dynamic range. For all the above reasons, MSCT has greater contrast and temporal resolution than CBCT.[27]

Additional differences shall be taken into account for a fair comparison between CBCT and MSCT. The latter is widespread in all developed countries and so more easily accessible, allows a better image quality for soft tissue visualization and can also be used for contrast-enhanced examinations. Conversely, CBCT is typically used for any type of dental and jaw disorders, except for neoplastic lesions where the administration of contrast agents and the assessment of the soft tissues are mandatory. The same observations can be applied to the ear and cervical studies, where MSCT is undoubtedly preferable to CBCT if a malignant lesion

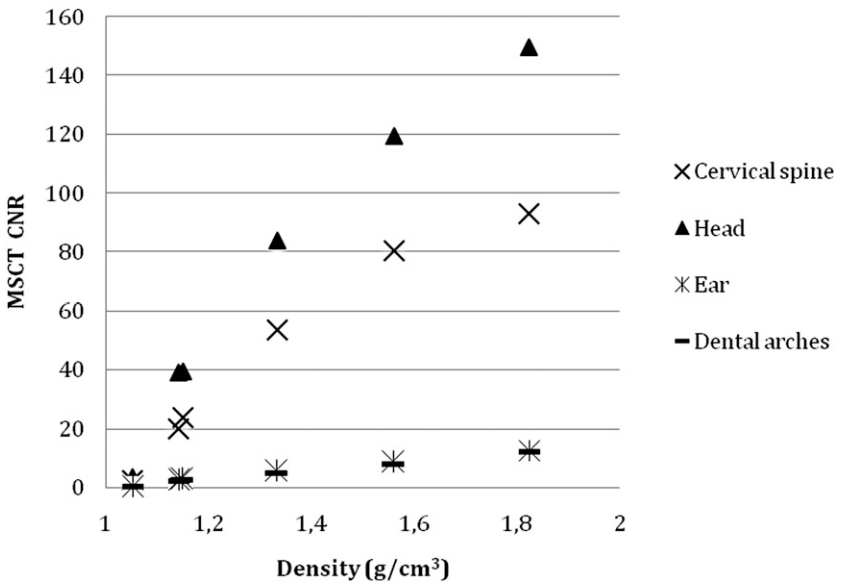

Figure 3 Multislice spiral CT (MSCT) contrast-to-noise (CNR) values as a function of the plugs density for each anatomical area.

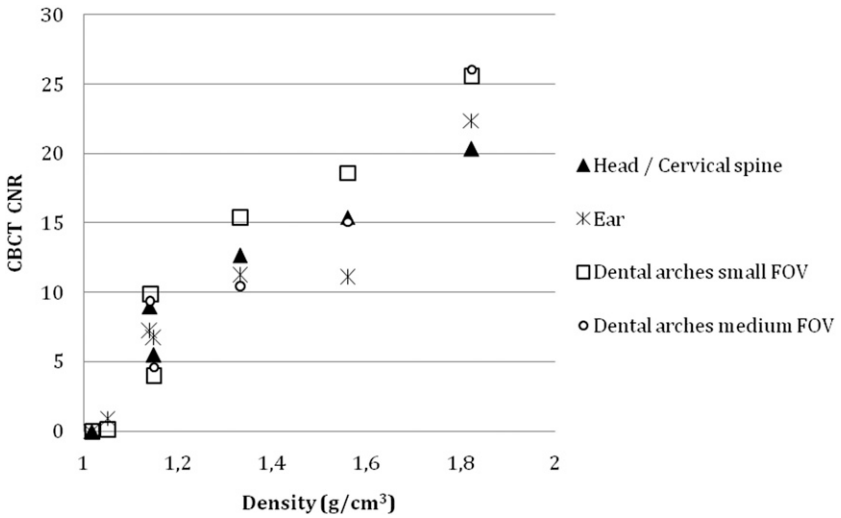

Figure 4 CBCT contrast-to-noise (CNR) values as a function of the plugs density for each anatomical area.

involving the skull base or the vertebral canal is suspected. When the head scan is carried out for orthognathodontic purposes, CBCT is recommended, but in the case of trauma and/or inflammation/neoplastic lesions, MSCT is mandatory.[15]

CBCT comes at lower mean technical and operating costs per procedure, approximately €60 and €150 for CBCT and unenhanced MSCT, respectively.[28,29] A disadvantage of CBCT is represented by its long scan time. This facilitates the presence of motion artefacts[30] and can negatively affect both the technical and clinical quality of the image compared with MSCT.

With two efficient CT techniques available for head and neck imaging, clinicians and radiologists must carefully evaluate—depending on the clinical query and anatomical structures under examination—whether to favour the reduction of radiation dose at the detriment of image quality, or better image quality at the cost of higher radiation dose. Finding a balance between benefit and potential harm to the patient is a critical point in the field of radiology.

The concept of irradiated fraction has long been debated. In our study, it does not represent the portion of a certain organ included in a specific FOV, but the percentage of the organ included in the head and neck area with respect to the total body amount of that same organ. Consequently, the irradiated fraction was 100% for salivary glands, thyroid gland, brain, extrathoracic airways and oral mucosa, whereas it was 13.3% for bone surface, 12.3% for bone marrow, 10% for oesophagus and 5% for skin, muscles and lymphatic nodes.[5,20–22] In case a different approach is used, the various organ irradiated fractions may vary, therefore the relative dosimetric values will not be comparable.

Organs and tissues receiving the highest organ dose were those located inside the primary beam and studied with high tube current–exposure time products. They were the thyroid gland in cervical spine scan and the eye lens, ossicular chain and muscles in ear scan.

In head scans, the dose to the thyroid gland—in comparison to the overall effective dose—showed a percentage value clearly higher in CBCT than MSCT (36.7% *vs* 21.1%). This is because in CBCT, the head scan is performed for orthodontic purposes, and all the soft tissues of the face must be included within the FOV. Therefore in CBCT, at least part of the thyroid gland is directly exposed to the primary beam, whereas in MSCT, it completely sits below the field of direct exposure. Consequently, the caudal positioning of the FOV becomes a critical point. Slight downward movement or rotation of the Frankfort plane[31,32] can lead to a significant increase of the dose to the thyroid, with an obvious increase of the effective dose. To reduce the patient's radiation dose in the case of CBCT with large FOV, the head should be slightly extended as to avoid the thyroid gland being affected by the primary beam. This does not jeopardize the correct execution of the examination since CBCT uses isotropic voxels, thus the volumetric data set can be oriented at any plane desired during the reconstruction process.[33]

In head and ear scans performed with MSCT, the dose percentage to the brain was twice that of CBCT. That was because in the MSCT head scan, the cranial positioning of the FOV affected the entire head, whereas it just barely included the frontal sinus in CBCT. In the ear scan, it was because the FOV of the MSCT was cranially 1 cm larger than the FOV of CBCT (6 *vs* 5 cm), including the pituitary gland in the radiation field. In the current study, bone marrow, salivary glands and remainder tissues were predominantly responsible for the effective dose in CBCT and MSCT ear scans. Zou et al[14] reported lower dose values for the salivary glands and remainder tissues in CBCT ear scan due to the use of a different CBCT unit with a smaller FOV (6 × 6 cm) that included mainly the brain in the primary beam, as well as the bone marrow.

In cervical scans, the thyroid gland was responsible for most of the effective dose (57.5% in MSCT and

Table 5 Effective dose of all anatomical areas compared to different diagnostic procedures and common everyday occurrences

Anatomical area	*Cervical spine*		*Head*		*Ear*		*Dental arches*		
Effective dose (μSv)	MS, 3409	CB, 247	MS, 1892	CB, 248	MS, 660	CB, 361	MS, 814	CBm, 689	CBs, 567
Time per capita background[a]	1 year	1 month	7 months	1 month	2.6 months	1.4 months	3.3 months	2.7 months	2.3 months
Attributable lifetime cancer risk[b]	41	3	23	3	8	4	1	8	7
Hours of airplane travel[c]	680	50	380	50	130	70	160	140	110
OPT	–	–	–	–	–	–	54	46	38
OPT + Ceph (2 projections)	–	–	90	12	–	–	–	–	–
Cervical spine (2 projections)	57	4	–	–	–	–	–	–	–
Chest (2 projections)	55	4	30	4	9	5	12	9	7

CB, CBCT; CBm, CBCT with medium FOV (12 × 8 cm); CBs, CBCT with small FOV (8 × 8 cm); Ceph, cephalometric radiography; FOV, field of view; MS, multislice CT; OPT, orthopantomography.
The effective dose of OPT, cephalometry (two projections), cervical spine (two projections) and chest (two projections) X-rays are considered 15,[34] 6,[34] 60[35] and 62 μSv,[36] respectively.
[a]Time to accumulate comparable natural background dose.[37]
[b]Lifetime attributable risk of cancer per 100,000 patients.[36]
[c]Ionizing radiation in an airplane travel. Cosmic radiation dose is considered 5 $\mu Sv\,h^{-1}$ at 12.000 m above sea level.[38]

71.8% in CBCT) because it was the only one highly radiation-sensitive organ (weight factor 0.04) with high irradiated fraction (100%) included in the primary beam. The lower thyroid dose percentage in MSCT depended on the bigger craniocaudal diameter of the FOV (18 *vs* 16 cm), producing higher dose to the brain, oesophagus and extrathoracic airway.

In dental arches scans, as reported in other studies,[5] the salivary glands (especially the parotid) were the organs mostly exposed to radiation because they were directly irradiated by the central X-ray beam. Nevertheless, the organs contributing to the most part of the effective dose were the thyroid glands due to a higher weight factor and irradiated fraction, and the remainder tissues due to the sum of the dose of four organs (extrathoracic airways, oral mucosa, lymphatic nodes, and muscles).

The only previous article estimating the effective dose in the head and neck area with NewTom5G CBCT was published by Dierckx et al.[13] They analyzed the ear using identical technical/geometrical CBCT parameters adopted in the current study, nevertheless MSCT delivered an effective dose six times higher than CBCT (and not twice as in our case). This is because of the marked difference in parameters between the two MSCT units, in particular 300 mAs and 140 kV *vs* 120 mAs and 120 kV in the current study.

When comparing the effective dose of NewTom5G and different CBCT units with similar FOVs,[9] NewTom5G fell within the middle range in head scan (249 μSv in the current study *vs* 46–498 μSv) and over the range in dental scan (565 μSv with small FOV and 688 μSv with medium FOV *vs* 69–453 μSv) due to different technical/geometrical parameters and hardware between the CBCT units.

Such major differences in patient dose highlight the importance of knowledge and optimization of the parameters during CBCT examinations. This reflects on image resolution because dose reduction leads to reduction in image quality.

The main limit of this study was that no repeated measurements were carried out since the use of a large number of TLDs, although improving the accuracy of dose calculation is a time consuming process. However in our series, the dosimetric values were given by the mean value of two measurements (a couple of dosemeters in each hole) performed during the same session.

Another weakness in our study was the use of CNR metric to compare protocols and scanners with different voxel sizes: smaller voxels do not receive as many photons as larger voxels, resulting in an intrinsic reduction of signal that leads to an increase in noise.

Finally, the effective dose of each anatomical area was compared with the radiation exposure resulting from common everyday occurrences and different diagnostic procedures; it is indeed interesting to notice significant dosimetric differences among the different scans (Tables 3 and 4) and their possible consequences (Table 5).

In conclusion, even though the current study was carried out on phantoms and thus the results could be slightly different in a clinical setting, it can be stated that:

(i) In the ear and dental arches imaging, CBCT was preferable to MSCT due to its lower radiation dose and significantly higher spatial resolution;
(ii) In the cervical spine and head imaging, the choice between CBCT and MSCT should depend on the clinical query. MSCT should be recommended when a high contrast resolution is required, despite the greater radiation exposure.

References

1. Brenner DJ, Hall EJ. Computed tomography—an increasing source of radiation exposure. *N Engl J Med* 2007; **357**: 2277–84. doi: https://doi.org/10.1056/nejmra072149

2. Nemtoi A, Czink C, Haba D, Gahleitner A. Cone beam CT: a current overview of devices. *Dentomaxillofac Radiol* 2013; **42**: 20120443. doi: https://doi.org/10.1259/dmfr.20120443

3. Nardi C, Borri C, Regini F, Calistri L, Castellani A, Lorini C, et al. Metal and motion artifacts by cone beam computed tomography (CBCT) in dental and maxillofacial study. *Radiol Med* 2015; **120**: 618–26. doi: https://doi.org/10.1007/s11547-015-0496-2
4. Casselman JW, Gieraerts K, Volders D, Delanote J, Mermuys K, De Foer B, et al. Cone beam CT: non-dental applications. *JBR-BTR* 2013; **96**: 333–53.
5. Ludlow JB, Ivanovic M. Comparative dosimetry of dental CBCT devices and 64-slice CT for oral and maxillofacial radiology. *Oral Surg Oral Med Oral Pathol Oral Radiol Endod* 2008; **106**: 106–14. doi: https://doi.org/10.1016/j.tripleo.2008.03.018
6. Suomalainen A, Kiljunen T, Käser Y, Peltola J, Kortesniemi M. Dosimetry and image quality of four dental cone beam computed tomography scanners compared with multislice computed tomography scanners. *Dentomaxillofac Radiol* 2009; **38**: 367–78. doi: https://doi.org/10.1259/dmfr/15779208
7. Okano T, Harata Y, Sugihara Y, Sakaino R, Tsuchida R, Iwai K, et al. Absorbed and effective doses from cone beam volumetric imaging for implant planning. *Dentomaxillofac Radiol* 2009; **38**: 79–85. doi: https://doi.org/10.1259/dmfr/14769929
8. Pauwels R, Beinsberger J, Collaert B, Theodorakou C, Rogers J, Walker A, et al. Effective dose range for dental cone beam computed tomography scanners. *Eur J Radiol* 2012; **81**: 267–71. doi: https://doi.org/10.1016/j.ejrad.2010.11.028
9. Ludlow JB, Timothy R, Walker C, Hunter R, Benavides E, Samuelson DB, et al. Effective dose of dental CBCT—a meta analysis of published data and additional data for nine CBCT units. *Dentomaxillofac Radiol* 2015; **44**: 20140197. doi: https://doi.org/10.1259/dmfr.20140197
10. Faccioli N, Barillari M, Guariglia S, Zivelonghi E, Rizzotti A, Cerini R, et al. Radiation dose saving through the use of cone-beam CT in hearing-impaired patients. *Radiol Med* 2009; **114**: 1308–18. doi: https://doi.org/10.1007/s11547-009-0462-y
11. Ludlow JB, Walker C. Assessment of phantom dosimetry and image quality of i-CAT FLX cone-beam computed tomography. *Am J Orthod Dentofacial Orthop* 2013; **144**: 802–17. doi: https://doi.org/10.1016/j.ajodo.2013.07.013
12. Cohnen M, Kemper J, Möbes O, Pawelzik J, Mödder U. Radiation dose in dental radiology. *Eur Radiol* 2002; **12**: 634–7. doi: https://doi.org/10.1007/s003300100928
13. Dierckx D, Saldarriaga Vargas C, Rogge F, Lichtherte S, Struelens L. Dosimetric analysis of the use of CBCT in diagnostic radiology: sinus and middle ear. *Radiat Prot Dosimetry* 2015; **163**: 125–32. doi: https://doi.org/10.1093/rpd/ncu117
14. Zou J, Koivisto J, Lähelmä J, Aarnisalo A, Wolff J. Pyykkö I. Imaging optimization of temporal bones with cochlear implant using a high-resolution cone beam CT and the corresponding effective dose. *Ann Otol Rhinol Laryngol* 2015; **124**: 466–73. doi: https://doi.org/10.1177/0003489414565004
15. Horner K, Armitt G, Bannard M. Radiation Protection: Cone Beam CT for dental and maxillofacial radiology. Evidence Based Guidelines 2012. Updated January 2017. Available form: http://www.sedentexct.eu/files/radiation_protection_172.pdf
16. Ekestubbe A, Gröndahl K, Gröndahl HG. Quality of preimplant low-dose tomography. *Oral Surg Oral Med Oral Pathol Oral Radiol Endod* 1999; **88**: 738–44. doi: https://doi.org/10.1016/s1079-2104(99)70018-1
17. Johns HE, Cunningham JR. *The physics of radiology*. 4th edn. Springfield, IL: Charles C Thomas Publisher Ltd; 1983.
18. Golikov VY, Nikitin VV. Estimation of the mean organ doses and the effective dose equivalent from Rando phantom measurements. *Health Phys* 1989; **56**: 111–5.
19. Scalzetti EM, Huda W, Bhatt S, Ogden KM. A method to obtain mean organ doses in a RANDO phantom. *Health Phys* 2008; **95**: 241–4. doi: https://doi.org/10.1097/01.hp.0000310997.09116.e3
20. Cristy M. Active bone marrow distribution as a function of age in humans. *Phys Med Biol* 1981; **26**: 389–400. doi: https://doi.org/10.1088/0031-9155/26/3/003
21. Borisov BK, Marei AN. Weight parameters of adult human skeleton. *Health Phys* 1974; **27**: 224–9.
22. Johnson, LC. Morphologic analysis in pathology. In: Frost, HM, ed. *Bone Biodynamics*: Little, Brown and Company. Boston, MA; 1964. pp. 543–654.
23. Valentin J. International Commission on Radiological Protection. Recommendations of the International Commission on Radiological Protection. 2007 ICRP Publication 103. *Ann ICRP* 37. Elsevier.
24. Edyvean S, Jones A. Measurement of the performance characteristics of diagnostic X-ray systems used in medicine: part III: Computed Tomography X-ray Scanners. IPEM Report 32—Part III. 2nd edn. York: IPEM; 2004.
25. Schneider CA, Rasband WS, Eliceiri KW. NIH image to ImageJ: 25 years of image analysis. *Nat Methods* 2012; **9**: 671–5. doi: https://doi.org/10.1038/nmeth.2089
26. Feldkamp LA, Davis LC, Kress JW. Practical cone-beam algorithm. *J Opt Soc Am A* 1984; **1**: 612–9.
27. Pauwels R, Beinsberger J, Stamatakis H, Tsiklakis K, Walker A, Bosmans H, et al. Comparison of spatial and contrast resolution for cone-beam computed tomography scanners. *Oral Surg Oral Med Oral Pathol Oral Radiol* 2012; **114**: 127–35. doi: https://doi.org/10.1016/j.oooo.2012.01.020
28. Saini S, Sharma R, Levine LA, Barmson RT, Jordan PF, Thrall JH. Technical cost of CT examinations. *Radiology* 2001; **218**: 172–5. doi: https://doi.org/10.1148/radiology.218.1.r01ja01172
29. Christell H, Birch S, Hedesiu M, Horner K, Ivanauskaité D, Nackaerts O, et al. Variation in costs of cone beam CT examinations among healthcare systems. *Dentomaxillofac Radiol* 2012; **41**: 571–7. doi: https://doi.org/10.1259/dmfr/22131776
30. Nardi C, Molteni R, Lorini C, Taliani GG, Matteuzzi B, Mazzoni E, et al. Motion artefacts in cone beam CT: an *in vitro* study about the effects on the images. *Br J Radiol* 2016; **89**: 20150687. doi: https://doi.org/10.1259/bjr.20150687
31. Pauwels R, Theodorakou C, Walker A, Bosmans H, Jacobs R, Bogaerts R, et al. Response to Letter to the Editor: comment on "effective dose range for dental cone beam computed tomography scanners". *Eur J Radiol* 2012;**81**:4221–4.
32. Morant JJ, Salvadó M, Hernández-Girón I, Casanovas R, Ortega R, Calzado A. Dosimetry of a cone beam CT device for oral and maxillofacial radiology using Monte Carlo techniques and ICRP adult reference computational phantoms. *Dentomaxillofac Radiol* 2013; **42**: 92555893.
33. Kiljunen T, Kaasalainen T, Suomalainen A, Kortesniemi M. Dental cone beam CT: a review. *Phys Med* 2015; **31**: 844–60. doi: https://doi.org/10.1016/j.ejmp.2015.09.004
34. Harris D, Horner K, Gröndahl K, Jacobs R, Helmrot E, Benic GI, et al. E.A.O. guidelines for the use of diagnostic imaging in implant dentistry 2011. A consensus workshop organized by the European Association for Osseointegration at the Medical University of Warsaw. *Clin Oral Implants Res* 2012; **23**: 1243–53. doi: https://doi.org/10.1111/j.1600-0501.2012.02441.x
35. Ben-Shlomo A, Bartal G, Mosseri M, Avraham B, Leitner Y, Shabat S. Effective dose reduction in spine radiographic imaging by choosing the less radiation-sensitive side of the body. *Spine J* 2016; **16**: 558–63. doi: https://doi.org/10.1016/j.spinee.2015.12.012
36. Smith-Bindman R, Lipson J, Marcus R, Kim KP, Mahesh M, Gould R, et al. Radiation dose associated with common computed tomography examinations and the associated lifetime attributable risk of cancer. *Arch Intern Med* 2009; **169**: 2078–86. doi: https://doi.org/10.1001/archinternmed.2009.427
37. Lin EC. Radiation risk from medical imaging. *Mayo Clin Proc* 2010; **85**: 1142–6. doi: https://doi.org/10.4065/mcp.2010.0260
38. Bagshaw M. Cosmic radiation in commercial aviation. *Travel Med Infect Dis* 2008; **6**: 125–7. doi: https://doi.org/10.1016/j.tmaid.2007.10.003